

Carbon Fluxes and Microbial Activities from Boreal Peatlands Experiencing Permafrost Thaw

M. P. Waldrop^{1*}, J. McFarland¹, K. Manies¹, M. C. Leewis¹, S. J. Blazewicz^{1,2}, M. C. Jones³, R. B. Neumann⁴, J. K. Keller⁵, L. Cohen⁶, E. S. Euskirchen⁶, C. Edgar⁶, M. R. Turetsky^{7†}, W.L. Cable^{8,9}

¹U.S. Geological Survey, Geology, Minerals, Energy, and Geophysics Science Center, Menlo Park, CA, USA 94025

²Physical and Life Sciences Directorate, Lawrence Livermore National Laboratory, 7000 East Ave, Livermore, CA, USA 94550

³U.S. Geological Survey, Florence Bascom Geoscience Center, Reston, VA, USA 20192

⁴Department of Civil and Environmental Engineering, University of Washington, Seattle, WA, USA 98195

⁵Schmid College of Science and Technology, Chapman University, Orange, CA, USA 92866

⁶Institute of Arctic Biology, University of Alaska Fairbanks, Fairbanks, AK, USA 99775

⁷Department of Integrative Biology, University of Guelph, Guelph, ON N1G 1G2, Canada.

⁸Geophysical Institute, University of Alaska Fairbanks, Fairbanks, AK, USA, 99775

⁹Alfred Wegener Institute, Helmholtz Centre for Polar and Marine Research, Potsdam, Germany

Contents of this file

Text S1 Electron shuttling capacity methods.

Figure S1. Species composition among the four sites at the Alaska Peatland Experiment

Figure S2. Soil temperatures (°C) in the three bogs

Figure S3. Cumulative net ecosystem exchange in permafrost plateau and collapse scar bog ecosystems

Figure S4. Cumulative fluxes of A) CO₂ and B) CH₄ from laboratory incubations of soils from young, intermediate, and old bog soil horizons.

Figure S5. Solid-phase electron shuttling capacity (ESC) in thermokarst bog soils.

Figure S6. Potential rates of soil enzyme activities

Figure S7. Estimates of methanogen, archaea, and bacteria abundance were made using quantitative PCR (qPCR) in the three bogs.

Figure S8. Concentration and isotopic data for CO₂ and CH₄ with depth in three different aged bogs

Figure S9. Output of the porewater isotope model with depth in three different aged bogs.

Table S1. Soil C and N concentrations of thermokarst bog soils

Introduction

This supporting information contains figures of plant community, climate, soil chemical, microbial, and flux data from the manuscript. Data are presented as figures here because results were presented as text in the article, or data were used in a biogeochemical model and results of the model were presented in the paper. Information related to how and when data were collected are presented in the methods of the main paper, except for the electron shuttling capacity methods, which are presented in detail here.

Text S1. Electron shuttling capacity methods.

Soils were oxidized overnight at 5 °C, homogenized using a food processor, added to 72-mL serum bottles and slurried with deionized water (3 g soil : 20 mL water). A total of 36 bottles were created for each soil horizon. Bottles were assigned to either chemically reduced or biologically reduced treatments. Soils were chemical reduced by adding 10 palladium-coated aluminum pellets to the slurries and replacing the bottle headspace with 99.9% H₂. Ten glass beads were added to the biologically reduced soils, which also had a H₂ headspace. Chemical reduction took place for 7 days at room temperature on a shaker table (150 rpm). On days 2 and 7, the bottles were opened in an anaerobic chamber (Coy Laboratory Products Inc., Grass Lake, MI, USA) and the pH of the chemically reduced slurries was adjusted to match the pH of the biologically reduced slurries using 0.5M HCl. At the end of the 7-day chemical reduction period, glass and palladium pellets were removed in the anaerobic chamber and the bottles were flushed with N₂ for 15 minutes. Bottles were incubated in the dark at 5 °C for 65 days.

On days 2, 10, 20, 35, 50 and 65, three bottles from each treatment were sacrificed for ESC measurements. In an anaerobic chamber, slurries were transferred to 50-mL centrifuge tubes which were removed from the anaerobic chamber and centrifuged for 5 minutes at 4000 rpm. The tubes were returned to the anaerobic chamber and the supernatant was filtered through pre-leached Whatman GF/D and GF/F filters. To determine the ESC of the dissolved phase, a 0.25 mL aliquot of the filtrate was added to 1 mL of 5 mM ferric iron complexed with nitriloacetic acid and vortexed for 1 minute. Fe(II) resulting from electrons shuttled from the dissolved phase was determined using ferrozine (0.1% ferrozine in HEPES buffer, pH=7.0). To determine ESC of the solid-phase organic matter, 15mL of 5 mM ferric iron complexed with nitriloacetic acid was added to the soil remaining in the 50-mL centrifuge tubes in the anaerobic chamber. The tubes were shaken vigorously and centrifuged a second time for 5 minutes at 4000 rpm. Fe(II) resulting from electrons shuttled from the soil was determined using ferrozine. The centrifuge tubes were dried to constant mass at 60 °C and to determine the dry mass of soil and volume of porewater. Solid-phase ESC was expressed as mmol e⁻ gdw⁻¹ after correcting for electron transfer from the porewater remaining in the peat used to measure solid-phase ESC. If organic terminal electron acceptor reduction was a dominant anaerobic process, we would expect that the biologically reduced treatment would show progressively higher solid-phase ESC over the course of the incubation period as the solid-phase organic matter gained electrons (Keller and Takagi 2013).

There was no evidence of ESC in the young, intermediate, or old bogs in any of the soil layers. Higher values reflect more reduced organic matter. Thus, if organic matter reduction was an important microbial process, the ESC of the biologically reduced soils would begin low (organic matter is oxidized) and increase to match the chemically reduced treatment as the

microbial community added electrons to the organic matter pool. This pattern is only seen in Core 1 of the basal layer in the young Bog. In all other cases, the organic matter is reduced in both the biologically and chemically reduced soils suggesting that organic matter reduction is not occurring over the course of the incubations. It is likely that organic matter was fully reduced during the 7-day chemical reduction period in both treatments.

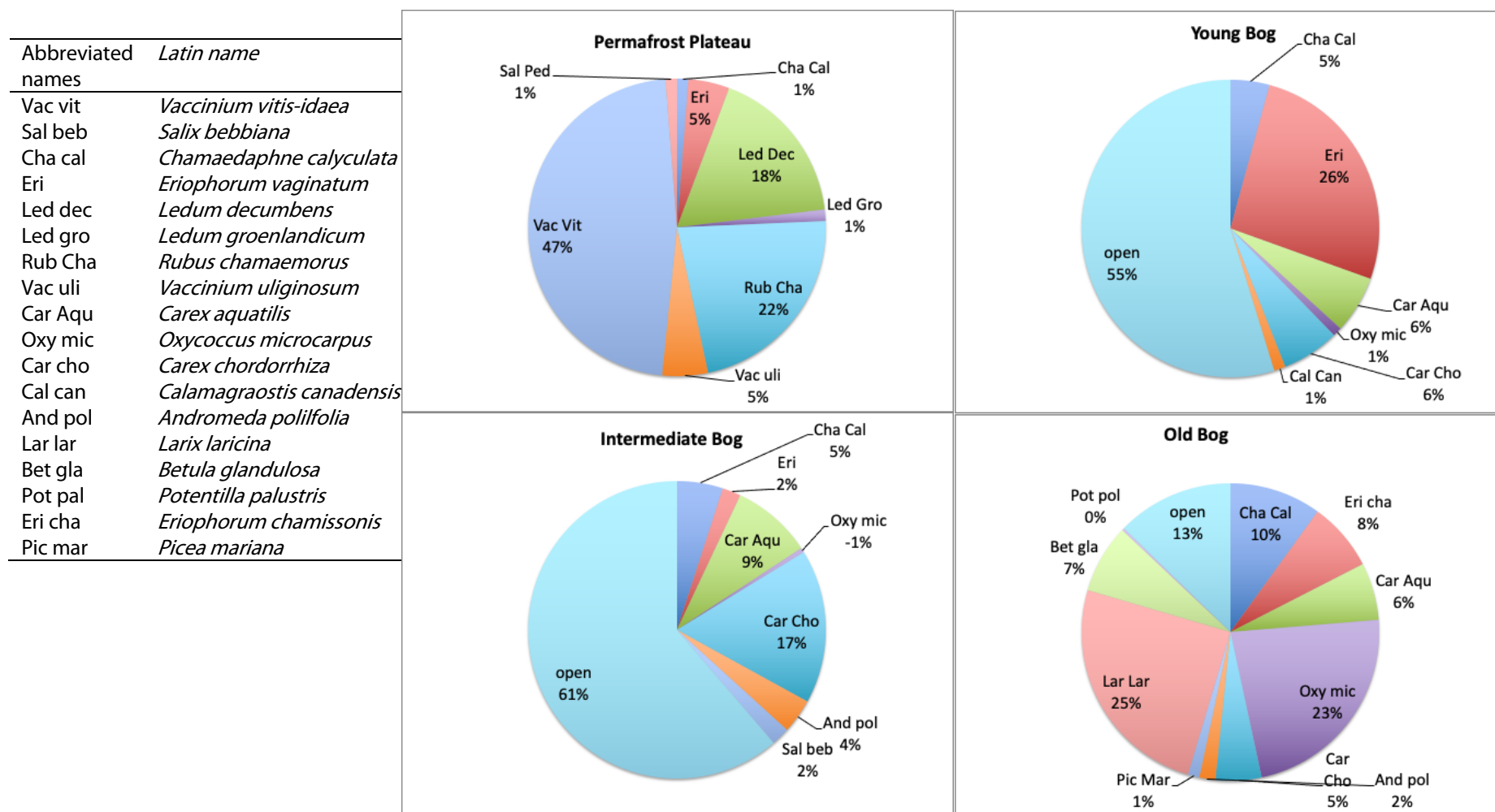
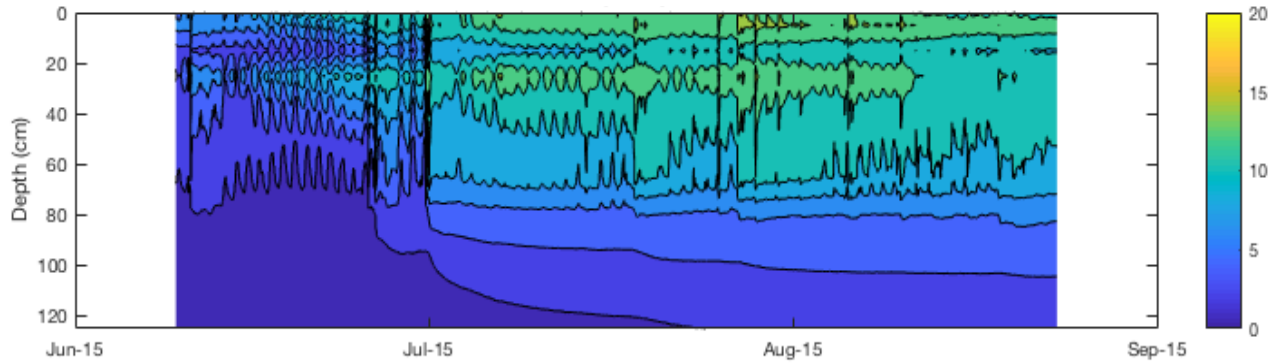
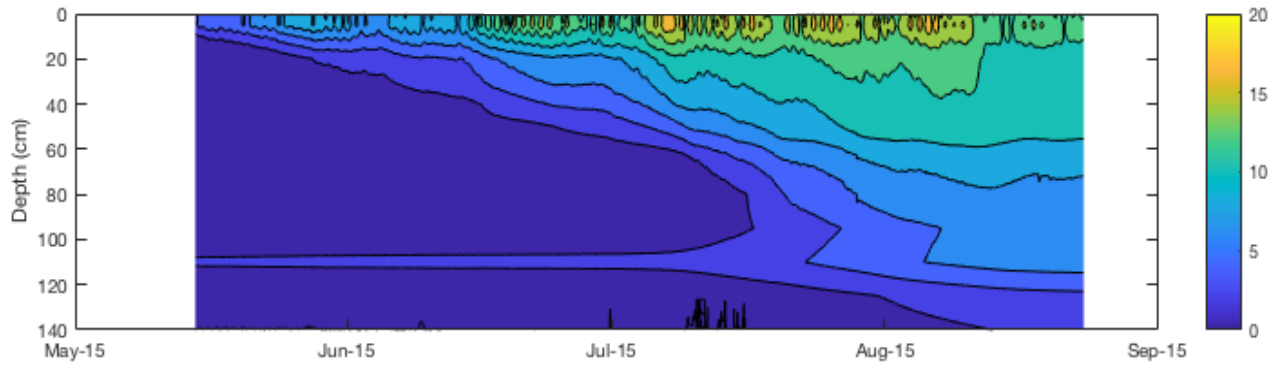


Figure S1. Species composition among the four sites at the Alaska Peatland Experiment (APEX). Pie charts indicate the % cover of individual vascular species among the research sites. 'Open' indicates area that was not covered by a vascular plant species so that % cover of all plant species is the actual percent cover measured in the field.

Young Bog



Intermediate Bog



Old Bog

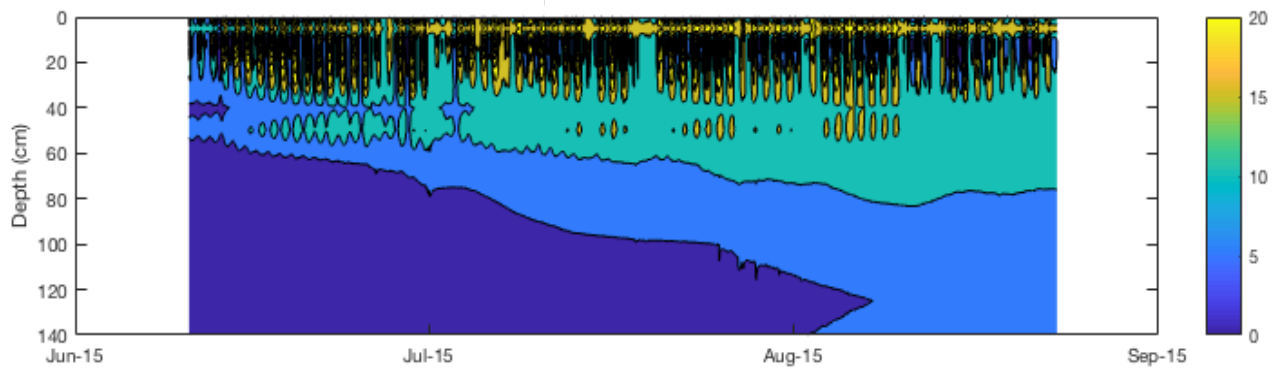


Figure S2. Soil temperatures (°C) in the three bogs. Soil temperatures were measured at fifteen intervals down to the bottom of each bog. Data were only available for 2015.

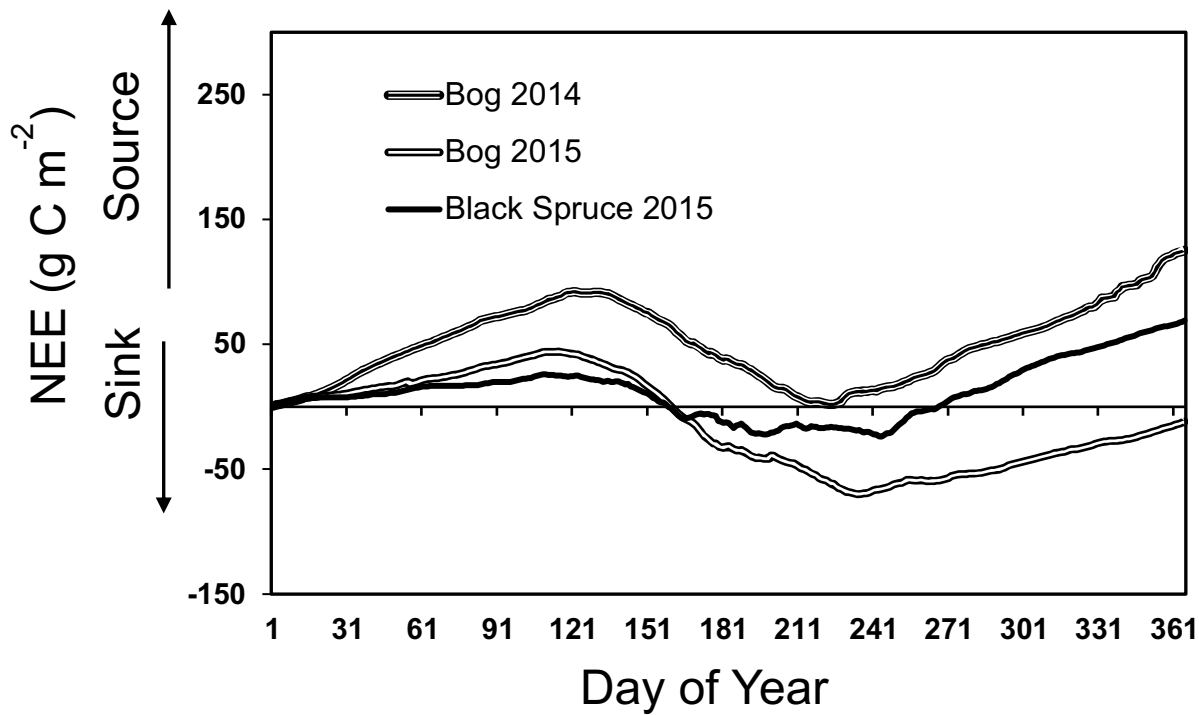
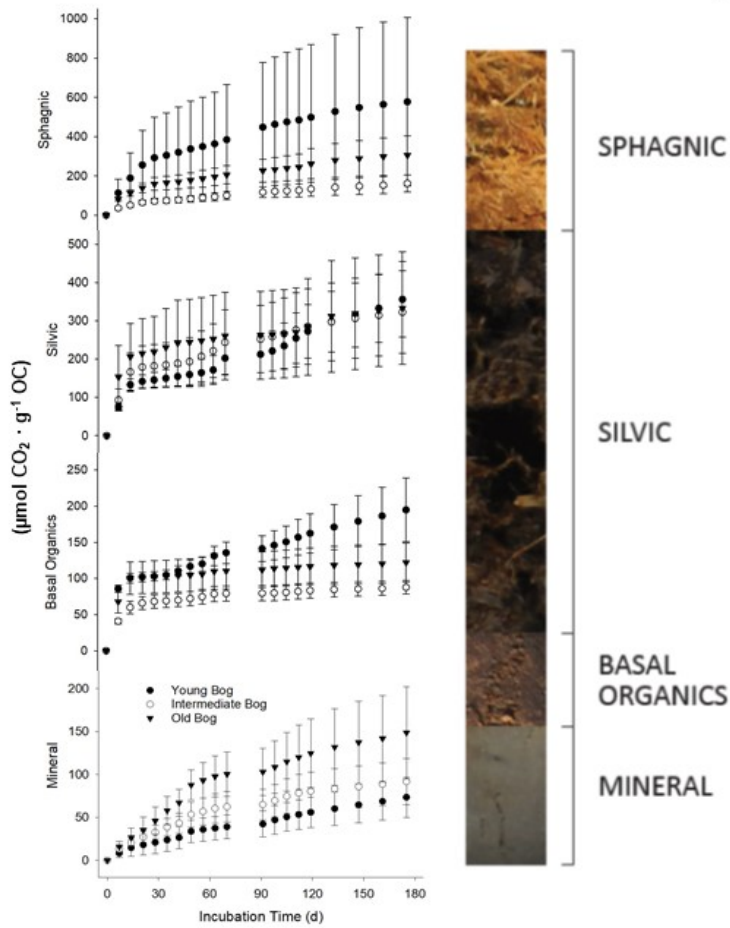


Figure S3. Cumulative net ecosystem exchange in permafrost plateau and collapse scar bog ecosystems. Cumulative net ecosystem exchange (NEE, g C m^{-2}) was measured with eddy covariance towers for 2014 and 2015 at the intermediate age collapse scar bog and for 2015 at the black spruce forest (the permafrost plateau). We did not have eddy flux towers in the young bog or old bog. Instrumentation issues prevented data collection during summer 2014 at the black spruce forest. Updated from Euskirchen et al. (2014).

A.



B.

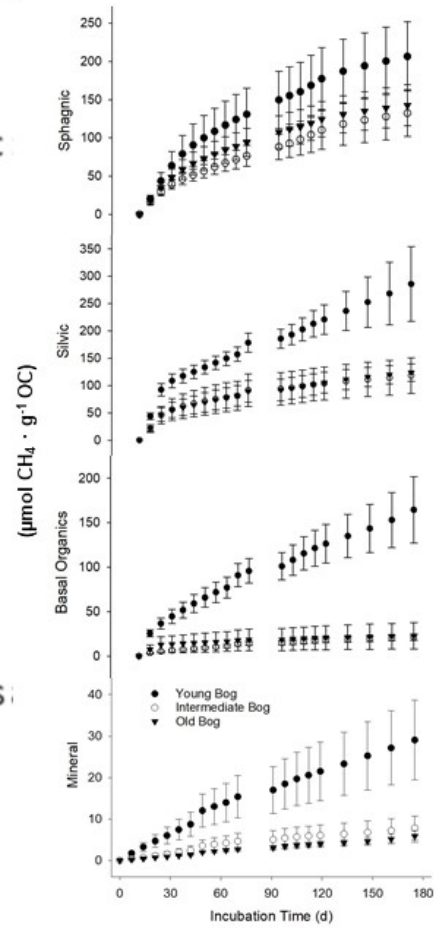


Figure S4. Cumulative fluxes of A) CO_2 and B) CH_4 from laboratory incubations of soils from young, intermediate, and old bog soil horizons. Images represent the relative depths of the different horizons (described in methods), but comparison of horizon depths among the three different aged bogs could not be completed due to compaction and lack of macrofossil data.

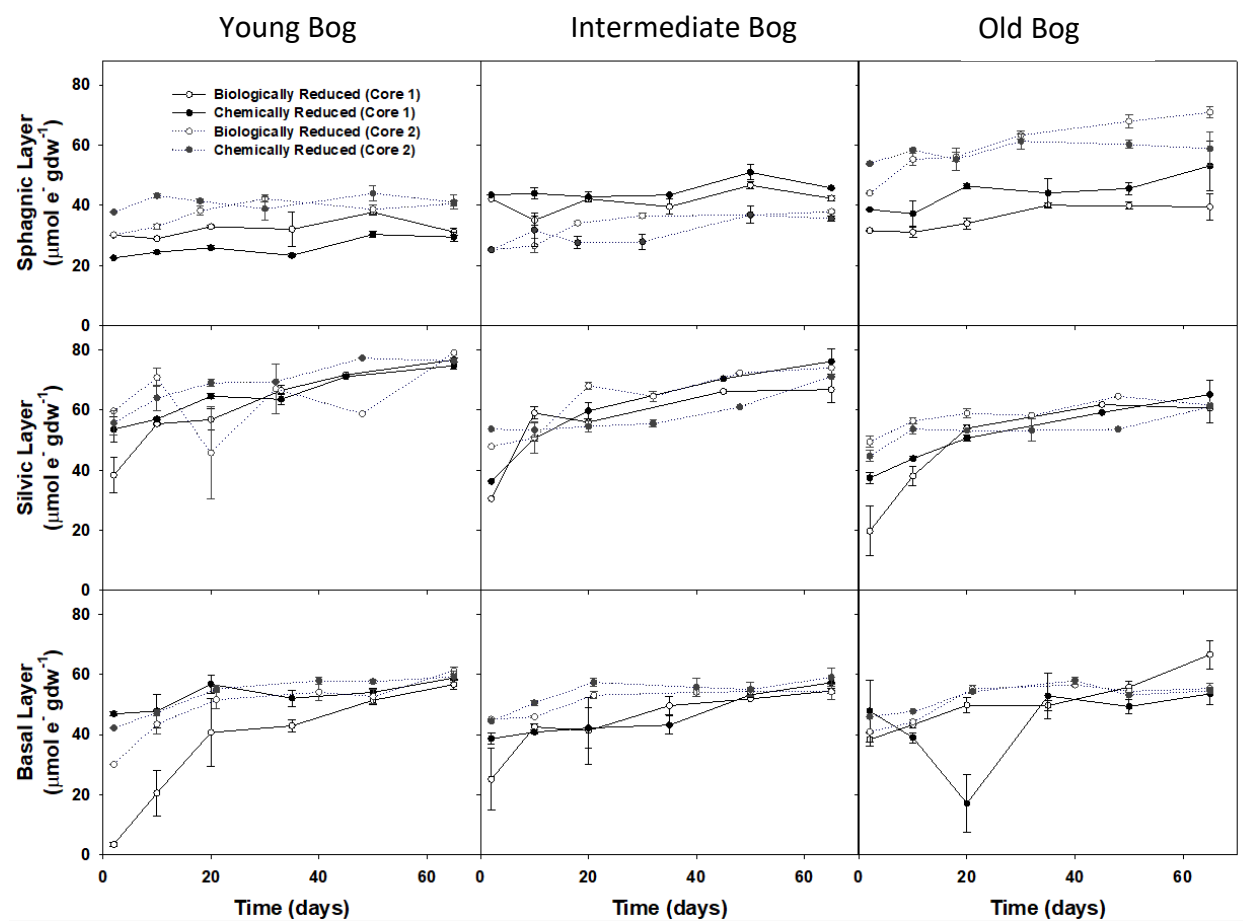


Figure S5. Solid-phase electron shuttling capacity (ESC) in thermokarst bog soils.

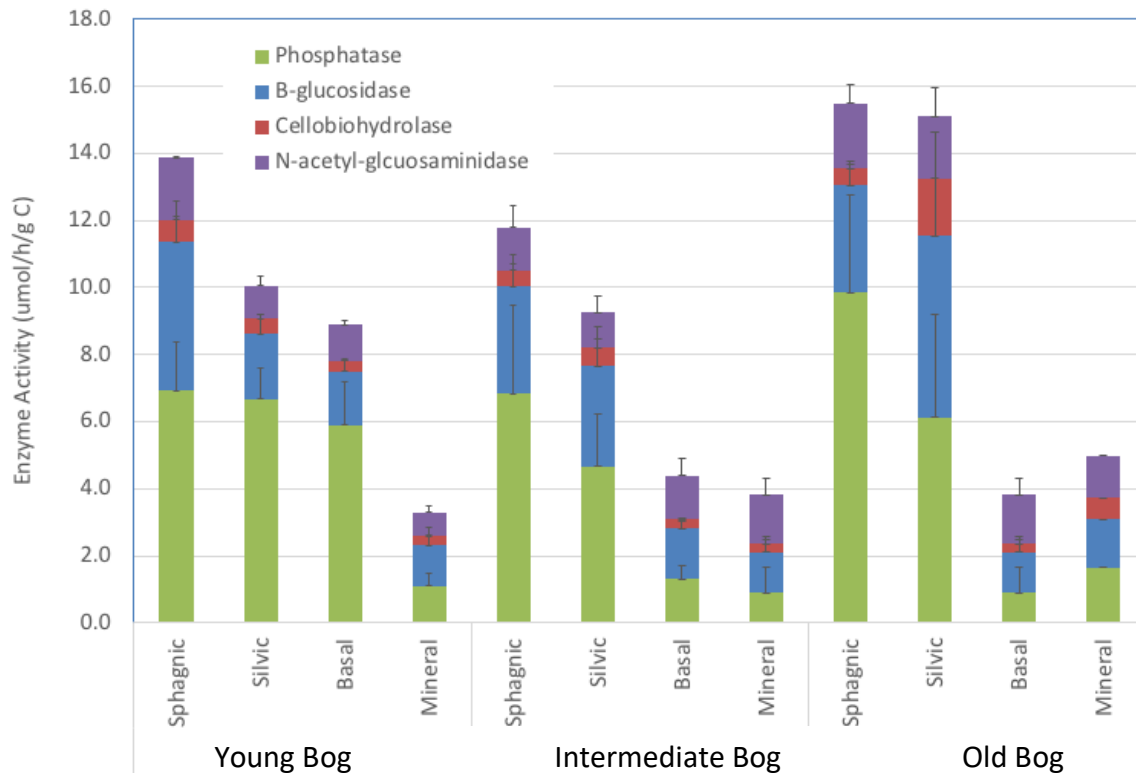


Figure S6. Potential rates of soil enzyme activities (mean \pm s.e., $n=3$). All enzymes except N-acetyl glucosaminidase showed a decline with depth (ANOVA main effect, $p < 0.0001$ for β -glucosidase and phosphatase, $p = 0.0006$ for cellobiohydrolase). Cellobiohydrolase also displayed a site \times depth effect in which the old bog was higher than the young bog in the silvic horizon and mineral horizon ($p = 0.0059$). Phosphatase displayed a site \times depth effect in which activity was higher in the basal layer of the young bog compared to the basal layer in the older bogs ($p = 0.0231$).

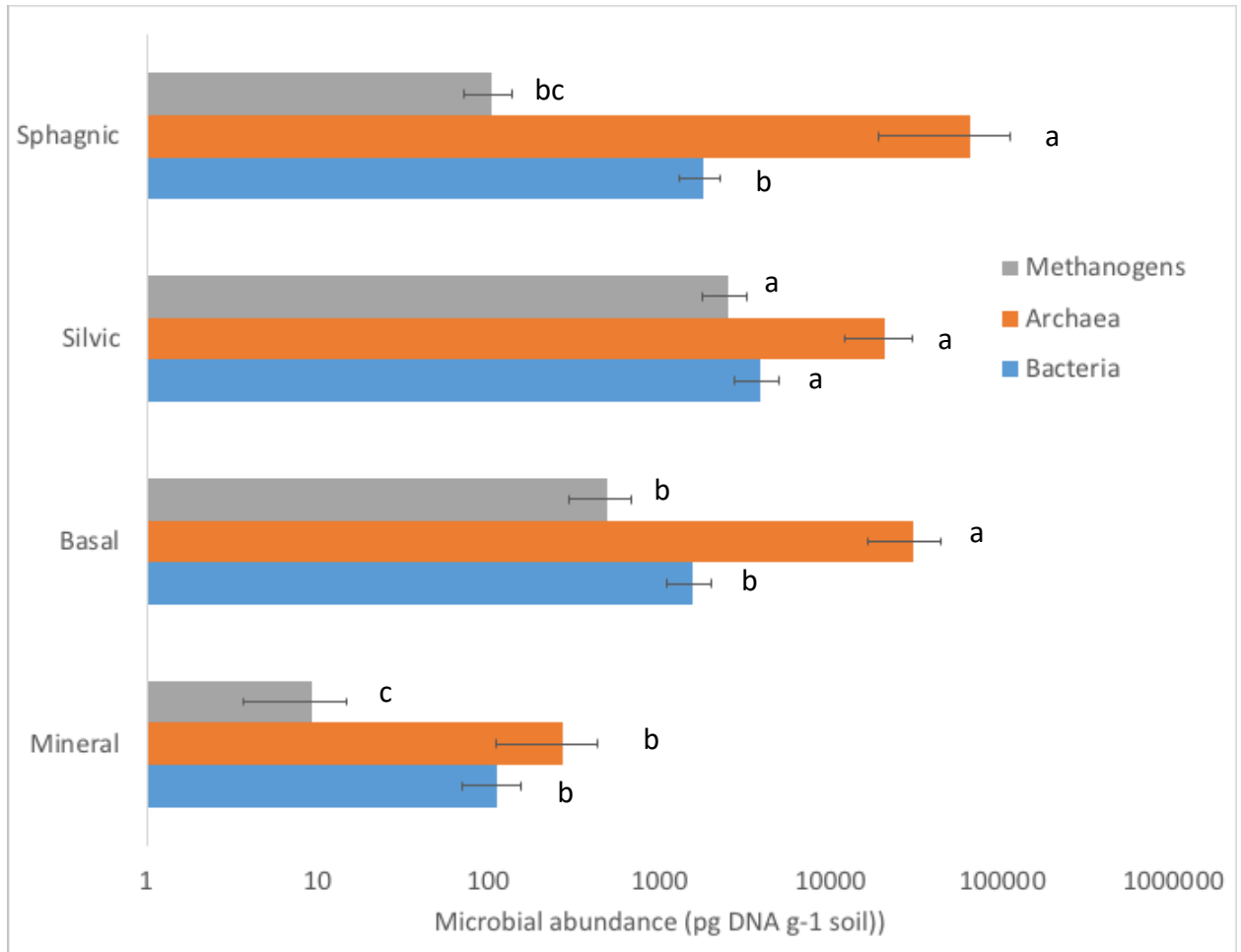


Figure S7. Estimates of methanogen, archaea, and bacteria abundance were made using quantitative PCR (qPCR) in the three bogs. Primers for bacteria, archaea, and methanogens were eub338 (f) and eub518 (r), arc300 (f) and arc 1000 (r), and mlas-mod-F (f) and mcrA-rev-R (r), respectively. Different letters indicate statistically significant differences in gene abundance among soil horizons.

Thermocycling parameters:

Bacteria: 95 °C for 5 min, followed by 35 cycles of 95 °C/1 min, 53 °C/0.5 min, 72 °C/1 min; and extension 72 °C/7 min.

Archaea: 98 °C for 2 min, followed by 30 cycles of 95 °C/0.5 min, 57 °C/0.5 min, 72 °C/1.5 min; and extension 72 °C/7 min.

Methanogen (*mcrA*): 95 °C for 4 min, followed by 30 cycles of 95 °C/0.5 min, 55 °C/45s, 72 °C/0.5 min; and extension 72 °C/10 min.

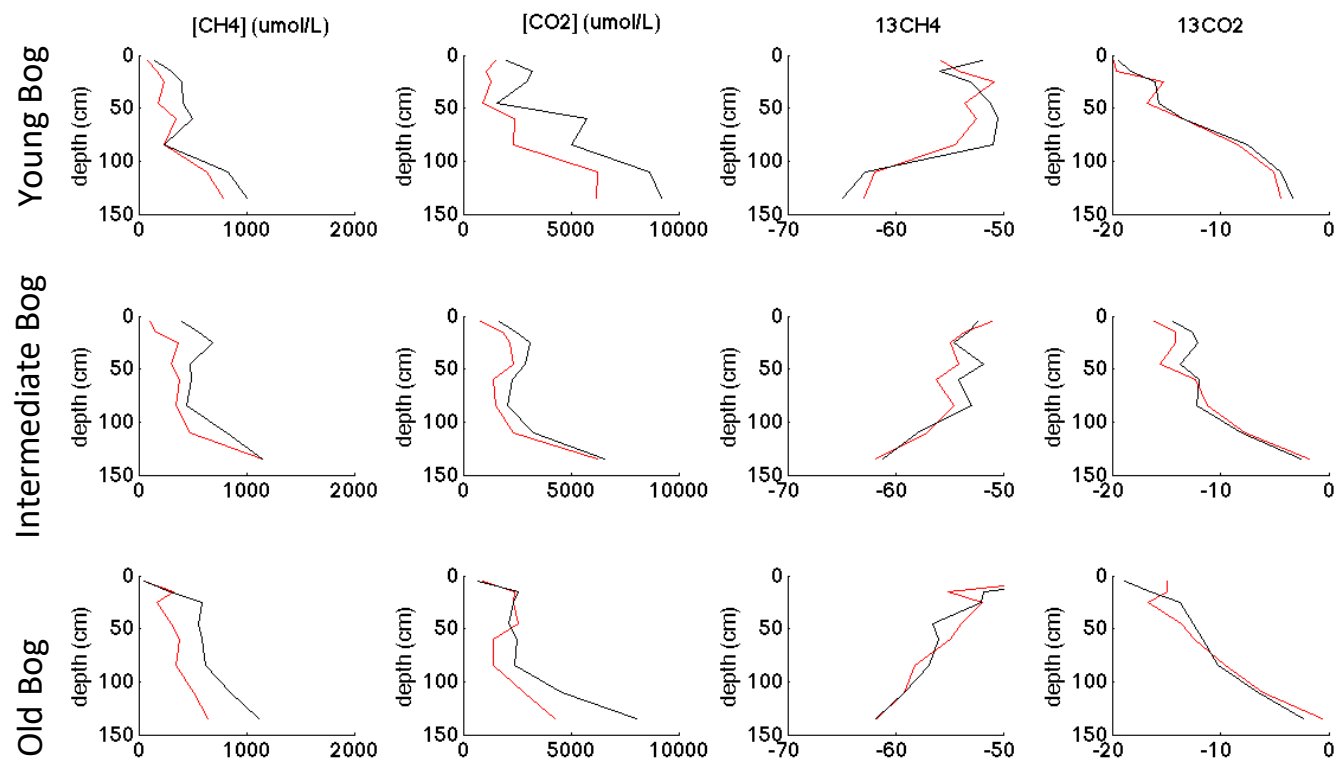


Figure S8. Concentration and isotopic data for CO_2 and CH_4 with depth in three different aged bogs. Red line indicates samples taken in July 2014 and black line indicates samples taken in August 2014. With increasing depth, dissolved $[\text{CO}_2]$ and $[\text{CH}_4]$ increased and $^{13}\text{CH}_4$ became more depleted while $^{13}\text{CO}_2$ became more enriched. The young bog had higher $[\text{CO}_2]$ compared to the older bogs.

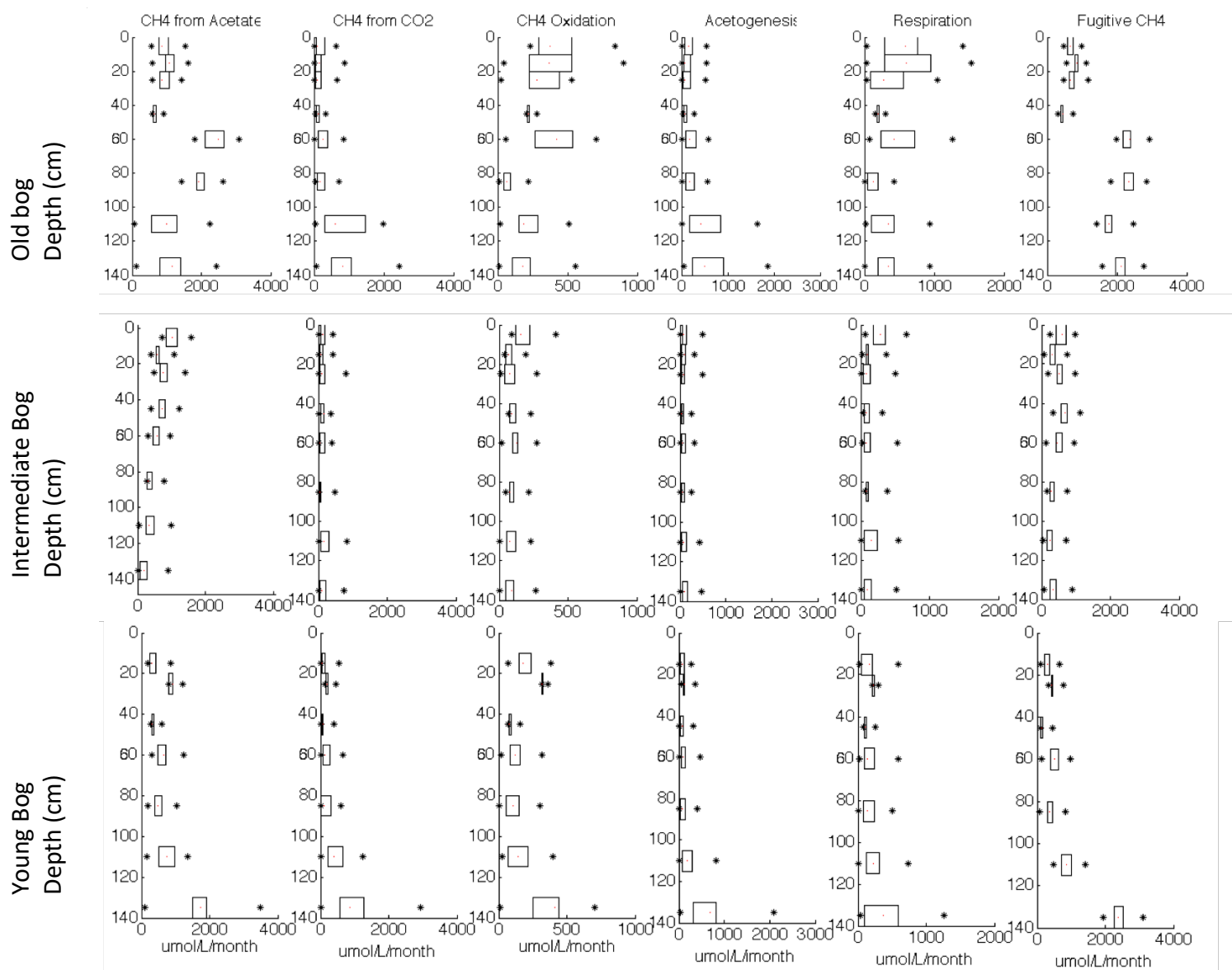


Figure S9. Output of the porewater isotope model with depth in three different aged bogs. The model calculates CH₄ production form acetate vs CO₂, CH₄ oxidation, acetogenesis, respiration and fugitive production of CH₄. Boxes represent 75% confidence intervals and stars represent 99% confidence intervals.

	Young Bog		Intermediate Bog		Old Bog	
	%C	%N	%C	%N	%C	%N
Sphagnic	38.5 ± 2.8 ^{bcd}	0.64 ± 0.02	43.2 ± 0.9 ^{ab}	0.68 ± 0.11	46.6 ± 1.6 ^a	0.88 ± 0.01
Silvic	39.6 ± 2.5 ^{bc}	1.46 ± 0.11	43.6 ± 1.1 ^{ab}	1.18 ± 0.14	39.8 ± 0.7 ^{bcd}	1.19 ± 0.02
Basal	30.8 ± 0.7 ^{cde}	1.62 ± 0.03	27.0 ± 1.8 ^{cdef}	1.51 ± 0.04	21.8 ± 0.14 ^{defg}	1.19 ± 0.22
Mineral	8.2 ± 1.1 ^{efg}	0.43 ± 0.06	5.5 ± 0.9 ^{fg}	0.28 ± 0.04	4.6 ± 0.14 ^g	0.25 ± 0.01

Table S1. Soil C and N concentrations of thermokarst bog soils. Values are means ± S.E (n=3). Superscripts indicate significant differences from a Tukey-Kramer HSD test. %C showed a significant site x depth interaction ($p < 0.0001$). % N showed a significant site effect and significant depth effect in which the young bog had higher % N than the other two bogs ($p = 0.004$). % N was highest in silvic and basal horizons, intermediate in the sphagnic horizon, and lowest in the mineral horizon ($p < 0.0001$). Superscripts are not shown in the % N columns as there was no site x depth interaction.